ELSEVIER

Brain Research Bulletin 75 (2008) 785–795

BRAIN RESEARCH BULLETIN

www.elsevier.com/locate/brainresbull

Research report

Bio-inspired sensorization of a biomechatronic robot hand for the grasp-and-lift task

B.B. Edin [c], L. Ascari [b], L. Beccai [a], S. Roccella [a], J.-J. Cabibihan [a], M.C. Carrozza [a,*]

[a] *ARTS Lab, Scuola Superiore Sant'Anna, viale Rinaldo Piaggio 34, 56025 Pontedera (PI), Italy*
[b] *IMT Lucca Institute for Advanced Studies, via S. Micheletto 3, 55100 Lucca, Italy*
[c] *Physiology Section, Department of Integrative Medical Biology, Umeå University, SE-901 87 Umeå, Sweden*

Available online 20 February 2008

Abstract

It has been concluded from numerous neurophysiological studies that humans rely on detecting discrete mechanical events that occur when grasping, lifting and replacing an object, i.e., during a prototypical manipulation task. Such events represent transitions between phases of the evolving manipulation task such as object contact, lift-off, etc., and appear to provide critical information required for the sequential control of the task as well as for corrections and parameterization of the task. We have sensorized a biomechatronic anthropomorphic hand with the goal to detect such mechanical transients. The developed sensors were designed to specifically provide the information about task-relevant discrete events rather than to mimic their biological counterparts. To accomplish this we have developed (1) a contact sensor that can be applied to the surface of the robotic fingers and that show a sensitivity to indentation and a spatial resolution comparable to that of the human glabrous skin, and (2) a sensitive low-noise three-axial force sensor that was embedded in the robotic fingertips and showed a frequency response covering the range observed in biological tactile sensors. We describe the design and fabrication of these sensors, their sensory properties and show representative recordings from the sensors during grasp-and-lift tasks. We show how the combined use of the two sensors is able to provide information about crucial mechanical events during such tasks. We discuss the importance of the sensorized hand as a test bed for low-level grasp controllers and for the development of functional sensory feedback from prosthetic devices.

Keywords: Bio-inspired systems; Tactile sensory system; Robotic hand; Robotic fingers; Grasping; Manipulation

1. Introduction

In this work we present a bio-inspired anthropomorphic artificial hand that mimics the biomechanical features and the sensory apparatus of the human hand. The rationale for this endeavor was multifold. First, such an artifact can be used as an experimental test object to explore control strategies proposed and tested in human subjects and to develop and evaluate novel ones. In addition, autonomous robots are likely to be required to handle objects designed primarily for human manipulation and as such may need to be equipped with anthropomorphic hands. Finally, and not less importantly, artificial hands may find a place in the rehabilitation of hand amputees and with patients congenitally lacking hands.

Humans use their hands for a range of behaviors including power grips, exquisitely fine manipulation, and communicative gestures. The versatility of the human hand relies both on its structure and its control. It displays an intricate biomechanical structure with many degrees of freedom and is endowed with a large number of specialized sensory endings residing in the skin, joints and muscles. Achieving our goal – an artificial hand that mimics the human hand – thus requires not only the mechanical design and implementation of an anthropomorphic hand [8], but also the implementation of a sensory system that compares with the human sensory system. It should be noted, however, that dexterous manipulation does not emerge by simply constructing an exact or improved replica of the human hand. Even simple manipulation tasks, such as a power grasp, require sophisticated control; indeed, simple grasps engage large parts of the human brain [17]. The coordinated and graceful lifting patterns observed in adults are not achieved in humans until 8–10 years of age [18,19]. Humans thus need almost a decade of daily

* Corresponding author. Tel.: +39 050 883416; fax: +39 050 883496.
E-mail address: carrozza@sssup.it (M.C. Carrozza).

0361-9230/$ – see front matter © 2008 Elsevier Inc. All rights reserved.
doi:10.1016/j.brainresbull.2008.01.017

practice before they master this apparently simple sensorimotor task.

The sensory system of the human hand serves a multitude of functions, e.g., nociception, thermal sensing, texture discrimination, stereognosis, and control of manipulation. Tactile sensor designers have often referred to the human mechanoreceptors of the glabrous (hairless) skin of the hand to draw inspiration [10,11,44,59]. In most cases however, the development of tactile sensors have focused on the individual sensor components rather than on complete systems for tactile sensing, and focused on general functionality rather than task-specific functions. In contrast, we have taken a biomechatronic approach, that is, we have concurrently addressed mechanical and sensor design. As such, we have focused in this study on the sensory signals pertaining to grasping tasks and specifically the signals required for grasp stability control during a prototypical task that forms an integrated part of most kinds of manipulation, i.e., grasping, lifting, and replacing an object [28,30].

1.1. Human grasping-and-lifting

The task of grasping-and-lifting objects and placing them back in the environment has been studied in humans in a large number of neurophysiological and behavioral studies in which subjects have lifted instrumented objects with or without simultaneous recordings of muscle activity (electromyography) and single afferent activity (microneurography) [33–36,57]. The behavioral organization of this task is characterized by both sequential and parallel coordination, i.e., it can be subdivided in sequential phases each characterized by a specific sensorimotor behavior and parallel activation of various muscle groups

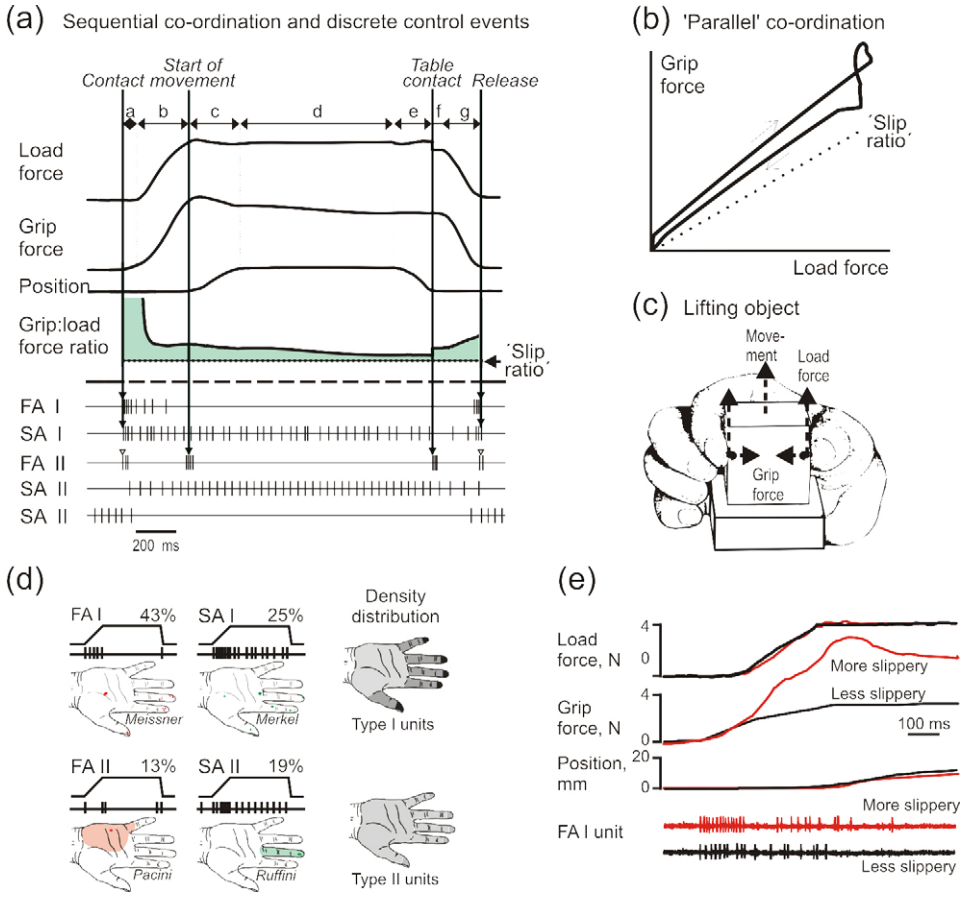

Fig. 1. (a) Schematic illustration of a lifting task during which a subject lifts an instrumented test object from a table, holds it in the air, and then puts it back, using the thumb and index finger. The tangential (load) force applied to the object to overcome gravity and inertia and the normal (grip) force are measured as well as the vertical movement. The grip:load force ratio needs to be above a certain minimum value to avoid slippage. The evolution of the task can be subdivided in a series of distinct phases: after contact with the object, demarcated by initial tactile responses, the grip force increases for a short period (a, *preload phase*) before the command is released for a parallel increase in grip and load force during isometric conditions (b, *load phase*). This parallel increase continues until the start of movement demarcated by burst responses in FA II afferents when the load force overcomes the force of gravity. The object is lifted to the intended position (c, *lifting phase*) by wrist and/or elbow flexion, and a static phase is reached (d, *hold phase*). After the replacement of the object (e, *replacement phase*) and table contact occurs (also demarcated by burst responses in FA II afferents), there is a short delay (f) before the two forces decline in parallel (g, *unload phase*) until the object is released (demarcated by tactile release responses). Adapted from Ref. [38]. (b) The grip and load force increases in parallel to achieve a grip:load force ratio above a certain slip ratio (dotted line). (c) Instrumented test object grasped with index and thumb. (d) Response and receptive field characteristics of the four types of low-threshold fast-conducting afferents from the glabrous skin. (e) Encoding of friction by a FA I unit with a receptive field on the fingertip. Superimposed force and position records from two trials with the same object but different surface materials. In the trial with the more slippery contact surface the unit discharged more vigorously and the subject adjusted the grip force with a delay of about 100 ms after the initial contact. Adapted from Ref. [34].

(Fig. 1a and b). Importantly, responses in tactile afferents mark transitions between phases [37,58].

The strategy represented by a parallel coordination of the grip and load forces in conjunction with a sequential organization of the specific sensorimotor conditions offers several advantageous features [27,30]. It allows, for instance, objects with unknown weights to be lifted since the load phase characterized by a parallel increase in grip and load forces may continue until lift-off has been detected. Similarly, manipulative tasks involving objects with different frictional properties are simplified because the required adjustment can be implemented by changing a single parameter, i.e., the ratio of the grip and load forces applied to the individual digit–object interfaces [16].

The mechanoreceptors known to be engaged in manipulative tasks can be subdivided into exteroceptors and proprioceptors. By definition, exteroceptors are primarily affected by external stimuli and are represented by tactile mechanoreceptors residing in the skin. Proprioceptors primarily encode mechanical events related to joint positions and muscle forces; they are traditionally represented by joint mechanoreceptors, muscle spindles and Golgi tendon organs. The subdivision into exteroceptors and proprioceptors is didactically useful but somewhat artificial given that typical exteroceptors respond to joints positions [13,14] and muscle spindles are exquisitely sensitive to external perturbations [48]. While classical proprioceptors are likely to provide crucial information necessary for appropriate reaching and grasping behaviors, there is no evidence that either muscle spindles or Golgi tendon organ afferents play important roles either during the prototypical-lifting task, or when the grasp is perturbed by external forces [20,46]. We will therefore focus entirely on skin mechanoreceptors and their role in the control of object manipulation.

The study of the neurophysiological properties of human skin mechanoreceptors was made possible with the advent of microneurography in the late 1960s [55]. With this technique a fine insulated tungsten electrode is inserted percutaneously into the nerve and carefully manipulated until the uninsulated 5–20 μm tip picks up signals from a single afferent nerve fiber originating in an individual peripheral receptor. Among all types of afferents supplying the human glabrous skin, the low-threshold, fast-conducting afferents are relevant for the current study. They belong to one of two main groups: slowly (SA) and fast adapting (FA) afferents (Fig. 1d). Whereas the SA afferents show a sustained response to indenting stimuli, FA afferents respond only when mechanical stimuli change. Both SA and FA can be further subdivided into types I and II afferents on the basis of their *receptive field* (RF) properties. By definition, the RF of an afferent corresponds to the skin area in which indenting stimuli evoke action potentials; the detailed topography of RFs could be very complex [26]. Type I afferents possess small and well-delineated RF whereas the RFs of type II afferents are large with poorly defined borders [56]. Each of the afferents innervates histologically defined structures which in part are responsible for the afferents' characteristic response properties. For instance, type I afferents in contrast to type II afferents innervate structures located superficially in the skin and this explains their different RF sizes. There are about 17,000 mechanoreceptive units innervating the glabrous part of the human hand and the majority (72%) are type I units [31]. The overall density increases in the proximo-distal direction and this increase can almost completely be explained by differences in the density of type I units (Fig. 1d). Instead of a smooth density gradient, there is a slight increase in innervation density from the palm to the main parts of the fingers and an abrupt increase from the main part of the finger to the fingertip.

When the fingertips make initial contact with an object, all types of afferents discharge although the response is most distinct in type I afferents (Fig. 1a). Similarly, all types of afferents discharge when the object is released from the grasp. While the initial contact activity provides important confirmation that the finger has made contact with an object, FA I afferents also seem to encode the frictional properties of the skin–object interface (Fig. 1e; [34]). Moreover, the initial contact information provides information about the spatial relationship between the tip of the digits and the object as well as the local curvature of the object in contact with the digits [24]. When the object starts to move or when it is replaced on the support, the mechanical transients evoke responses in the sensitive FA II afferents (Fig. 1a). These transients may have been caused by vibrations due to small lateral sliding movements between the object and the table. Importantly, the time of lift-off indirectly provides information about the object's weight and allows subjects to adjust the forces applied to the object during the actual behavior but also to parameterize subsequent manipulative actions with the same object since the lifting drive must be appropriately adjusted to match the weight of the object to allow smooth vertical lifting movements [30].

The importance of the tactile afferents in releasing the sequence of coordinated motor behaviors characteristic of the lift-and-hold task is illustrated by the behavior of humans with digital anesthesia. With anesthesia and without visual control, the phase from contact to the initiation of the load phase is significantly prolonged presumably because contact has not been confirmed by the tactile sensors [33]. Likewise, under digital anesthesia, subjects may fail to notice that a lift-off takes place and accordingly may continue to increase the vertical force until some other sensory system indicate the lift-off [38]. Except for the initial contact phase, the load and grip force increase and decrease in parallel during manipulative tasks (Fig. 1b). If the grip force is too low with respect to the load force, the object will slip. A parallel coordination of the grip and load forces thus ensures grasp stability [58]. The human tactile system plays an important role in adjusting the grip:load force ratio to allow a certain safety margin against slippage (Fig. 1a). As noted above, the discharge in FA I units reflects the frictional conditions at the digit–object interfaces. Adjustments to new frictional conditions are evident in a change in the grip:load force ratio within 100 ms after the initial contact (cf., Fig. 1e). This adjustment is usually sufficient for establishing an adequate safety margin. If, however, an overt or incipient slip occurs during the manipulative task this is promptly signaled by FA I and SA I units and the corrective action that results in increased grip:load force ratio commences in about 70 ms [34]. Importantly, while these corrective actions ensure long-term grasp stability, in most situ-

ations the mechanisms are too slow to prevent slippage if overt slips occur at all engaged digits. Nevertheless, taking the human performance as a reference, the design goal was to provide a reaction time to slippage of ≤70 ms for the integrated system of sensors, mechanisms, and control.

Only limited information about how various features of mechanical stimuli impinging on the skin are encoded by skin afferents is available. In general, stronger stimuli, e.g., larger forces, indentations or more rapid changes give rise to higher discharge rates, i.e., some stimulus features are encoded by the discharge rate in individual afferents [15,41,42]. In addition, larger stimuli evoke responses in more afferents, i.e., stimulus strength and spatial properties may be encoded in population codes [23]. Moreover, it has recently been proposed on the basis of microneurographic experiments that the very first spikes in ensembles of human skin afferents may encode complex mechanical events such as the direction of fingertip force and the shape of the surface contacting the fingertip [29].

1.2. Basic requirements for a bio-inspired tactile system

From the short review above regarding the normal physiology of grasping activities in humans, it is possible to identify the minimum requirements of a bio-inspired tactile system that can fulfill the functional requirements of its biological counterpart with respect to prototypical grasp-and-lift actions. In short, the tactile sensory system of an artificial hand must have the possibility to detect:

- contact and release between the fingertip and the object;
- object take-off and replacement to the environment; and
- slippage between the fingertip and the object.

Other functions of the physiological sensory system such as providing information about the local shape at contact points and overall object shape were thus outside the primary design goals.

2. Methods and materials

2.1. The biomechatronic hand

We have exploited robotic and microengineering technology to design and fabricate the building blocks of an underactuated biomechatronic hand [7]. The architecture of the hand comprises an embedded actuator system, an artificial 'proprioceptive sensory system' (position and force sensors), an exteroceptive sensory system, and an embedded low-level control unit. The biomechatronic hand has five digits (thumb and four fingers) with cylindrical phalanges (Ø 16, 14 and 12 mm and lengths 45, 25 and 22 mm for the proximal, middle and distal phalange of each finger, respectively) of aluminum alloy material attached to a central palm (95 mm × 105 mm × 40 mm; Fig. 2c). A mechanism that permitted self-adapting grasping without active control of the hand [47] was exploited to mimic human grasping behavior [39]. This was implemented by actuating the flexion of all phalanges of each digit via a cable pulled by a single DC motor. The antagonistic action for extension was implemented by a torsional spring embedded in each finger joint. The motor for thumb adduction and abduction was located inside the palm while the motors for the movement of the fingers were housed inside the forearm of the robot to which the hand can be attached, or could be placed in a socket worn by an amputee in prosthetic applications.

The bio-inspired sensory system consists of *proprioceptors* and *exteroceptors*. While the artificial proprioceptive sensors were designed to mimic their biological counterparts by providing information about both joint positions (by Hall effect sensors in each joint) and actuator forces (tensiometers on the cables), the exteroceptive system was designed to primarily convey information crucial for an adequate sequential coordination, that is, to provide information about contact between the object and the fingertip and between the object and the environment. The exteroceptive system was instantiated by designing flexible on–off contact sensors and three-axial force sensors.

2.2. Fabrication and characterization of contact sensors

To detect the contact between the hand and the environment, the design goal was to make the on–off contact sensors sensitive enough to emulate the mechanoreceptors of the human hand. It was estimated that 90% of the SA I and the FA I mechanoreceptors get excited to a stimulus of 5 mN [32]. In terms of

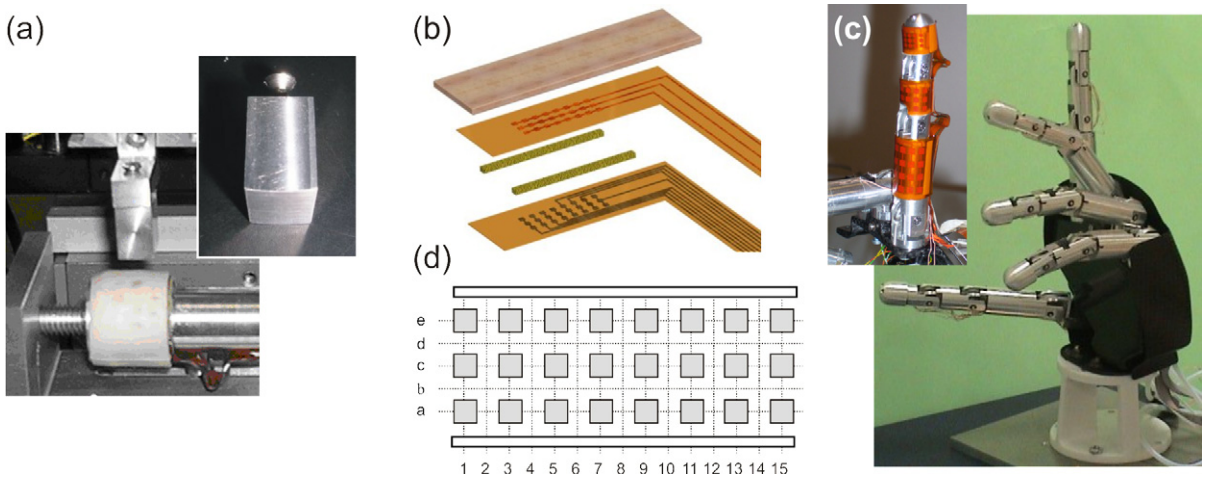

Fig. 2. (a) The aluminum probe interfaced with the characterization equipment and the on–off sensor mounted on a cylindrical support with same dimensions as the distal phalange of the robotic hand (Ø 12 mm); enlarged view of the probe (dimensions 9 mm × 6.55 mm × 15 mm). The surface that came into contact with the sensor had a small positive curvature (30 mm^{-1}; cf., inset). (b) The 24 taxel contact sensor comprised two Kapton® layers with embedded copper electrodes (1 mm × 1 mm at a distance of 1.4 mm) spaced by two layers of foam and with an upper 1 mm thick silicone layer; (c) The index finger of the five-fingered hand with tactile contact sensors mounted on the three phalanges and the biomechatronic five-fingered hand. (d) The coordinate system for the force application sites: 1–15 columns and a–e rows.

pressure, the 5 mN stimulus was applied through a von Frey hair with a diameter of 0.27 mm [25]. Therefore, contact activation <0.087 N/mm^2 represents the design goal for contact sensors development.

The sensors were designed and fabricated in layers that could be assembled and wrapped around the external surface of the mechanical structure of the hand. These sensors consisted of sensitive areas embedded in a flexible structure also used for carrying the wires with signals. The sensors that were mounted on the cylindrical digits of the biomechatronic hand were obtained from LF9150R Pyralux (DuPont, Wilmington, DE, USA) by a photolithography process. Pyralux consists of a 127 μm thick Kapton® sheet with a 35 μm layer of copper (305 g/m^2) on one side. The contact sensor was composed of two layers of Pyralux with a copper layer patterned by photolithography using a photoresist coverlay (by DuPont). On both layers an array of copper electrodes and lines for external connection were applied. When a force was applied to the contact sensor, the two Kapton® layers came closer and beyond a certain force level the copper electrodes on the two circuits come into contact. The sensors were assembled by positioning 2-mm thick strips (8 mm × 2 mm) of polyurethane foam between the two layers (Fig. 2b). The foam spacers allow the Kapton® layers to return to their initial states once any external force was removed. The sensor array, having a compliant silicone (GLS 40, Prochima s.n.c., Italy) outer layer (1 mm in thickness; Fig. 2b), encompasses 24 tactile elements (taxels) having a square geometry with dimensions of 1 mm × 1 mm (Fig. 2d).

In the human hand, the highest density of the tactile units is found in the fingertip [26,31,32]. Due to the anthropomorphic shape of the biomechatronic hand, the distal phalanx was the smallest link of the fingers. A matrix of 8 × 3 contact points was therefore designed for the fingertip, another 8 × 3 matrix for the middle phalange and an 8 × 4 matrix for the proximal phalange (Fig. 2c). Each finger could thus be equipped with a total of 80 flexible on–off contacts but for assessing their functional properties, contact sensors were mounted on the distal phalanges only.

Static characterization of the contact sensor array was obtained by mounting the contact sensor array on a cylindrical aluminum structure whose radius was the same as the distal phalange of the artificial hand (Ø 12 mm; Fig. 2a). Load was applied to the sensor through a six-components load cell (ATI NANO 17 F/T, Apex, NC, USA) mounted in an experimental test bench by exploiting three micrometric translation stages with crossed roller bearing (M-105.10, PI, Karlsruhe, Germany). The latter allowed the positioning of the loading structure on the tested sensor. Accurate positioning in the normal direction was further obtained by a servo-controlled nanometric translation stage (111-1DG, PI, Karlsruhe, Germany). Signals coming from the contact sensors array were acquired at the rate of 10 kHz and stored digitally; the acquisition board was a National Instruments PC-6032E and the software interface was developed in Labview 7®.

The force required to activate individual taxels was measured (threshold tests) as well as the force when the probe was retracted and the taxels again were deactivated. Hysteresis was defined as the difference between the onset and offset forces.

Threshold tests were performed by means of the probe shown in Fig. 2a. Its dimensions and curvatures were chosen to be similar to commonly grasped objects such as apples or glasses, in contrast to small objects such as needles or buttons. Error in sensor localization of the applied loading stimulus was identified by performing tests with the same aluminum probe with or without a 7-mm thick polyurethane layer (Poly 74-45 from Polytech Development, PA, USA). The measurements were performed by applying an increasing load on the contact sensor and by recording the force at which each area, with a different configuration, was activated in the on state. The distance between the point of application of the load and the centroid of the activated sensor electrodes patch was used to indicate the positioning error.

Spatial resolution is the minimum measurable distance between two different taxels that can be detected. The spatial resolution depends on, but does not coincide with, the spacing between two taxels fixed by the technology and materials used. In order to detect the spatial resolution of the sensor two cylindrical brass probes (Ø 1 mm; not illustrated) were used. These probes were interfaced to the loading system and used to load the sensor in the normal direction when the two-probe distance varied from 1 to 10 mm in 1 mm steps.

2.3. Fabrication and characterization of three-axial force sensors

The force sensor was primarily designed to measure three components of force generated at the contact points between an external object and the finger. The design goal was to satisfy the requirements of detecting perpendicular and tangential forces generated at mechanical transients. The strategy chosen was to develop a three-axial force sensor with sufficient bandwidth to correspond to both SA and FA tactile afferent, i.e., 2–400 Hz. As such, the designed sensor was not intended to directly emulate any particular mechanoreceptor type.

Indeed, all types of biological mechanoreceptors are essentially force sensors as they are all capable of detecting forces when the skin is compressed [4,29]. In functional terms, to fulfill the specific role of FA II afferents, the sensors should be able to detect the start and end of an object's vertical movement. Moreover, a three-axial sensor could be used to measure the force components applied normal to and tangential to a surface and hence allow computation of the grip:load force ratio [8].

The force sensor structure was analyzed and designed by means of FEA tools (ANSYS® 5.7) in order to identify the maximum strain levels and to choose the appropriate strain gauge elements. The actual sensor mounted at the fingertips was based on an aluminum alloy flexible structure. In order to detect the three components of an applied force, three metal-based strain gauges (N3K-06-S022H-50C, Vishay Micro-Measurements, Vishay Intertechnology Inc., PA) were attached to the root of each tether along the three axis of the sensor itself (see Fig. 3a). Three additional strain gauges were used for temperature compensation. The sensor was integrated at the tip of the distal phalanx (Fig. 3c).

The final aim of the tests on the force sensor was to measure its ability in detecting force changes. To this end the sensor was characterized statically, dynamically, and in term of noise.

The experimental test bench for force sensor characterization consisted of two main modules (Fig. 2a): the loading system and the distal phalange of the finger integrating the three-axial force sensor. The loading system was the same as the one used for the experiments on the contact sensors but now interfaced to a different probe consisting of a sphere (Ø 1 mm) fixed to a brass cylindrical support (inset of Fig. 3b). The six-components load cell (ATI NANO 17 F/T, Apex, NC, USA) (cf., Fig. 3b) was fundamental for characterizing the three-axial force sensor since it allowed the measurement and acquisition of both magnitude and direction of the force applied to the sensor. This experimental set-up made it possible to avoid force and torque components caused to misalignment between the loading structure and the sensor under test [54].

The first stage of the test bench used for static characterization was the electronic circuit for signal conditioning and temperature compensation and it consisted of a typical Wheatstone bridge. Strain gauge signal conditioning included three precision instrumentation amplifiers for accurate, low-noise differential signal acquisition with low offset voltage drift and excellent common-mode rejection (INA 126PA Burr-Brown, Texas Instruments, TX, USA). The three amplified signals were acquired with a DAQ card (NI 6036E, from National Instruments, TX, USA) at the rate of 10 kHz. A graphical user interface was developed in Labview 7® in order to sample the three sensor output signals contemporarily to the load cell signals. The static characteristics of the three-axial force sensor were determined by applying a set of three known static loads (∼1, 2, and 3 N) along each of x, y and z directions (cf., Fig. 3d) and recording the signals from each strain gauge for 5 s.

The test bench used for the noise and dynamic characterization of the sensor was the same as the one used for the static measurements described above, but the sampling rate was 40 kHz. Noise measurements were done over the whole signal chain, including the sensor and the acquisition electronics. The power spectral density of the noise was measured, as well as its root-mean-square (RMS) value by means of Matlab™ Signal Processing and System Identification toolboxes.

The approach used for extracting the frequency response of the three-axial force sensor consisted in stimulating the sensor by means of an impulsive stimulus in order to excite all the vibrational modes of the structure. The stimulus was obtained by means of a steel sphere (Ø 6 mm) falling on the sensor from a height of 29 cm along the x direction (cf., Fig. 3d); this principally excited the center strain gauge. The stimulus was modeled as an ideal impulse since this approximation did not have any consequences in the determination of the resonant frequencies.

The ability of the three-axial force sensor to detect force changes was tested in two experiments: induced slippage experiments and grasp-and-lift experiments.

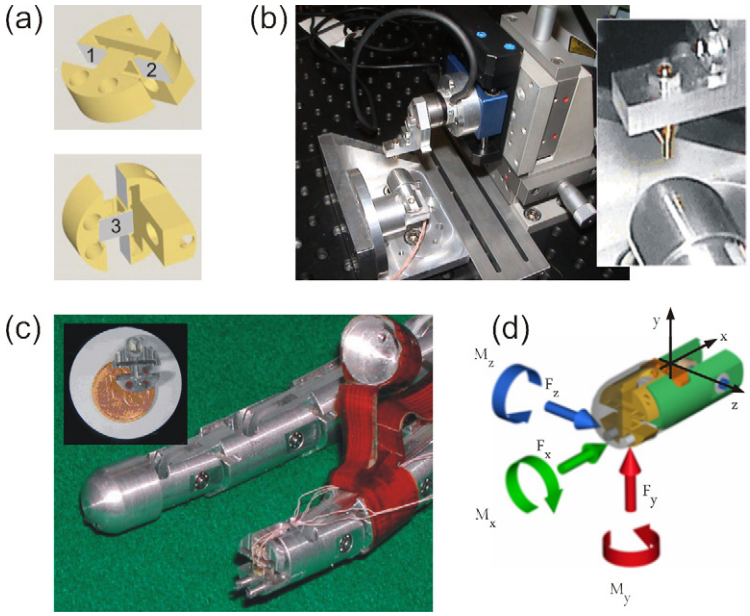

Fig. 3. (a) Sensor 3D model with indicated tether position of right (1), left (2) and center (3) strain-gauges. (b) Test bench sensor depicting the picture. A six-components load cell (linear forces and torques) was attached to a micrometric translation stage that allowed precise positioning of the test probe (inset). (c) Sensor integration at the distal phalange of the artificial hand. Inset allows size comparison with a €50-cent. (d) Sensor coordinate reference systems and applied loads for calibration.

In the slippage experiments, a robotic finger with an embedded three-axial force sensor was loaded with a force normal to the palmar surface of the fingertip. The loads were 1.4 and 3.8 N to mimic different grip forces. While this normal load was applied, the contact plate was moved tangential to the surface of the fingertip (cf., Fig. 3d), and consequent outputs from the sensor and the ATI load cell were recorded.

Grasp-and-lift experiments were carried out using cylindrical objects weighing 200–400 g (see inset of Fig. 6c). A simple open-loop control was used to sequentially (1) grasp the cylinder, (2) wait for 5 s, (3) apply a vertical lifting movement for a duration of 250 ms, (4) hold the cylinder in the air for 2 s, (5) replace the cylinder on the support, and finally, (6) release the object. Sensor signals, conditioned with the same electronics described in the previous section and load cell signals were sampled and acquired (with the same DAQ card NI 6036E) at 10 kHz by using a Labview 7® graphical user interface.

3. Results

The main issues addressed in this study were related to the sensory system performance, and in particular if the implemented system was able to fulfill the functional requirements of a prototypical-lifting task, that is, to detect critical mechanical transients that occur during such tasks.

3.1. On–off contact sensors

The spatial sensitivity profile of the contact sensor revealed that the pressure required to activate at least one of the contacts of the sensor was less than 0.015 N/mm^2 in most of the contact surface (Fig. 4a), a result well within the target activation threshold of 0.087 N/mm^2. It was always possible to activate a single contact and accordingly, the minimum distance between two probes to be detected was 2 mm. The difference between the pressure at which at least one contact sensor signals onset and subsequent offset when the pressure was released averaged <0.001 N/mm^2 ($7.3 \pm 3.8 \times 10^{-4}$ N/mm^2; mean ± S.D.). The results were the

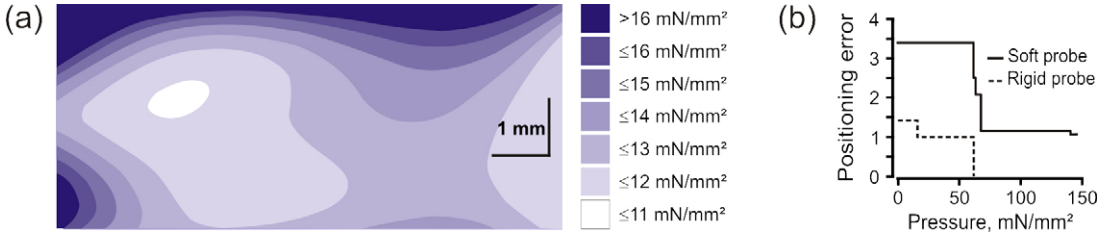

Fig. 4. (a) Spatial contact sensor sensitivity profile. The minimum pressure required to activate at least one of contact sensor electrodes was measured with the sensor wrapped around the artificial fingertip. The threshold within the whole displayed area was $13.3 \pm 0.45 \times 10^{-3}$ N/mm^2 (mean ± S.D.) measured with a probe with a 58.5 mm^2 surface area (cf., Fig. 2a). The 'finger pad' corresponds to the central part of the area. (b) Localization of center of stimulus application defined as the spatial mean of the activated electrodes of the contact sensor when the center of the probe was located midway between four electrodes. With the uncovered aluminum probe the error became zero once all four sensors were activated, that is, at 0.062 N/mm^2. When the same probe was covered with a 7-mm thick soft polyurethane layer a larger and non-symmetrical set of electrodes were recruited within the force range: the center of the probe could be determined with an error of <1.2 mm at a pressure of 0.062 N/mm^2.

same whether the force was applied for 2 or for 5 s. Accordingly, hysteresis was insignificant.

To estimate the error in the localization of the stimulus center, an aluminum probe with a contact surface measuring 57 mm^2 (Fig. 2a), uncovered and covered with a 7 mm thick soft polyurethane layer, was located midway between four electrodes. The center of pressure could be estimated from the geometrical center of the activated sensors. With the uncovered probe the error became zero once all four sensors were activated, that is, at 0.062 N/mm^2 (Fig. 4b). With the probe covered by the soft polyurethane surface, more sensor electrodes were recruited, and within the force range tested the probe did not activate a symmetrical set of electrodes; yet the center could be determined with an error of less than 1.2 mm at a pressure of 0.062 N/mm^2.

3.2. Three-axial force sensors

The raw outputs from all strain gauges during static characterization were linearly related to the loads (Fig. 5a). Thanks to the mechanical structure of the sensor it was possible to obtain a quantitative estimation of F_x, F_y and F_z components of the applied load through an appropriate combination of output from the strain gauges. The calibration curves (Fig. 5a) demonstrated that the detection of stimuli along the x direction relied only on the central strain gauge, while to measure stimuli along the y and z directions, combinations of the left and right strain gauges signals had to be computed.

The noise levels were low (e.g., Fig. 6). Estimating the noise from the RMS of the sensor output was justified by the observation that the noise power spectrum was broad and had an evenly spread power. The RMS of the calibrated forces was measured rather than that of the strain gauge outputs. It was found to be virtually independent of the load magnitudes, normally distributed, and were 0.019, 0.0079 and 0.0088 N along the x, y and z directions, respectively.

The shape of the frequency response of the sensor matched the one predicted from the theoretical simulations (Fig. 5b). The mechanical resonance frequency of the sensor was predicted by FEM analysis to be 2.5 kHz and was measured to be 2.7 kHz. The same resonance frequency was observed in measurements of absolute displacements during impulse stimuli. An additional resonance peak was predicted at around 380 Hz and was observed at 389 Hz. This peak was due to the particular strain gauges embedded in the sensor; they were primarily sensitive to the relative strain rather than to absolute displacement. Virtually the same frequency response curves were obtained from all three sensor channels.

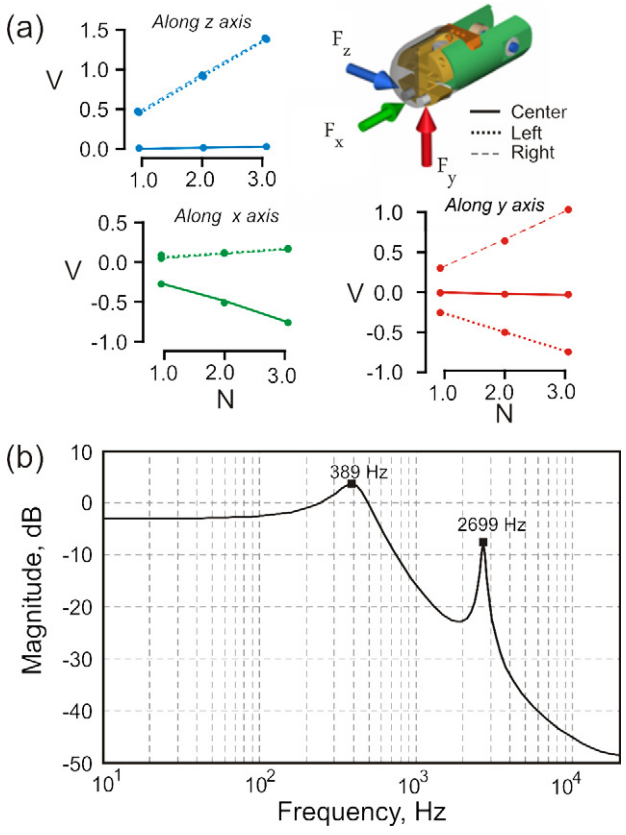

Fig. 5. Characterization of the static and dynamic response properties of the three-axial force sensor. (a) Linear responses were observed when forces were applied along to the x-, y- and z-axis, respectively. (b) Frequency response of the central strain gauge, normalized with respect to the total energy of the stimulus (the other two channels showed virtually identical response curves). The two resonance peaks were explained by the properties of the strain gauges (at 389 Hz) and the mechanical resonance frequency of the structure (at 2699 Hz).

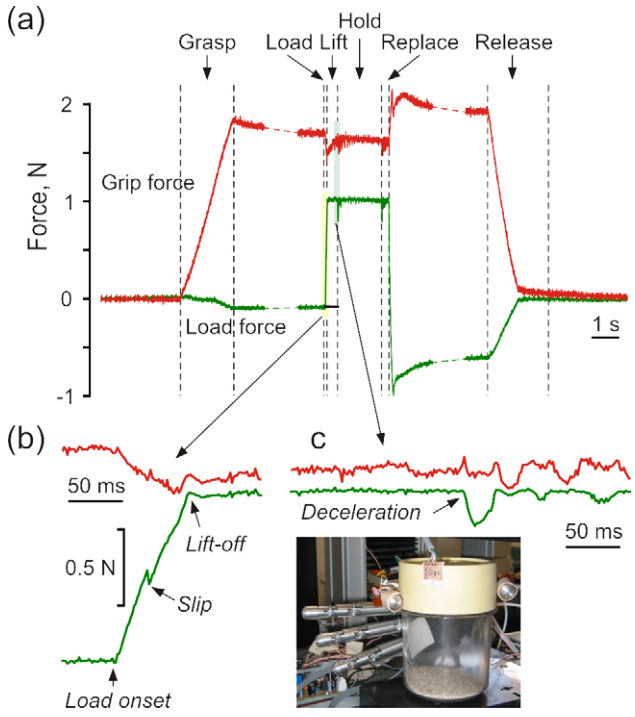

Fig. 6. Grasp-and-lifting trial. (a) The biomechatronic hand was controlled to grasp the cylindrical object (see inset in (c)) and after a few seconds delay, the hand was lifted vertically at 25 mm/s, held in position for 2 s, and then again lowered to the support whereupon the grasp was released. Both a slip that occurred during the start of the vertical movement (b) and the transient deceleration indicating the beginning of the hold phase (c) were clearly discernable in the recorded force signals and correctly detected within 10 ms.

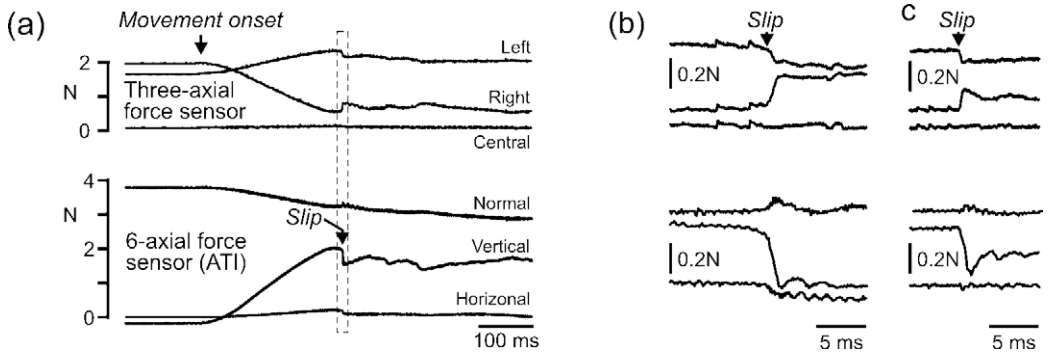

Fig. 7. Slip detection. (a) A robotic fingertip with an embedded three-axial force sensor was held horizontally in contact with a plate that could be moved vertically. Once the contact plate started to move, the vertical force recorded by the six-axial ATI force sensor increased until slippage occurred. The time period indicated by the rectangle is shown at a higher temporal resolution in (b) which indicates that the slippage was obvious also in the left and right sensor elements of the three-axial force sensor. An additional example of a slip event is shown in (c).

3.3. Detecting force changes

The ability of the three-axial force sensor to detect phase transitions was qualitatively assessed by engaging the sensor-equipped robot hand during a simple grasp-and-lift task (Fig. 6). The expected mechanical events during the task, e.g., contact, load force increase, deceleration of object after lift-off (Fig. 6c), etc., as well as an accidental slippage event during the load phase (Fig. 6b) were clearly represented in the force readings and would all be detected within less than 10 ms (cf., CUSUM methodology described below and Fig. 8).

In Fig. 7 are shown the calibrated signals from the strain gauges recorded while an instrumented object in contact with the fingertip with the embedded three-axial force sensor was subjected to linear traction (the initial normal force was 3.8 N). The increased force tangential to the fingertip (i.e., the 'vertical' force of the contact object) was primarily recorded by the left and right channels of the three-axial sensor. Once the tangential force reached the slip force a sudden break of the vertical force increase was observed and a concomitant change in the outputs of the three-axial sensor (high temporal resolution in Fig. 7b). Numerous additional examples of such slips were observed (e.g., Fig. 7c), indicating that slips would be easily detected using the three-axial sensor.

In case of slippage, sudden force changes occur only when the static (μ_S) and dynamic friction (μ_D) between two surfaces material are different (cf., [3]). Given a certain ratio μ_S:μ_D (and that neither μ_S nor μ_D depend on the normal force), the magnitude of such force changes at slippage depends on the normal force. In short, it should be easier to detect a slippage when the μ_S:μ_D ratio is large and the normal force is high than when both are small. The usefulness of the three-axial force sensor for detecting force changes depends on its sensitivity, frequency response and noise (RMS error).

It is possible to estimate the expected time required before a sudden unexpected change can be detected. As an example, assume that the sensor signal of a certain mean value, m, is sampled at an appropriate rate, f, and has the normal distribution $N(m, \text{S.D.})$. Then the deviation from the mean obviously would have the distribution $N(0, \text{S.D.})$. Let us sum the deviations in a moving window of w samples; the distribution of this sum is $N(0, \text{S.D.}\sqrt{w})$. Assume further that the recorded force changes by ΔF at time t_0 and that this results in a change ΔS in the sensor signal. For each sample following t_0 the cumulative sum will thus on average increase by ΔS. The average number of samples until the cumulative sum deviates more than a certain criterion value, C, can then simply be computed as $n = C/\Delta S$ (and the corresponding latency would be n/f). For more thorough descriptions of jump detection and cumulative summation techniques, see Ref. [1].

Fig. 8a exemplifies this detection method for three different step sizes corresponding to 0.5, 1.5 and 2.5 times the RMS observed for F_x readings of the three-axial force sensor. The simulated sensor signals were generated by filtering step increases of different amplitudes and thereby veraciously emulating responses of the three-axial force sensor (cf., Fig. 5b), adding noise corresponding to the estimated RMS and finally 'sampling' the signals at 2 kHz. The cumulative sums in moving 100 ms windows for the respective step size crossed a boundary that corresponded to falsely detecting a force change on average once an hour. The latency to detection depends, of course, on the size of the force step (Fig. 8b). The size of the force step that results from a slip, in turn, depends on both the μ_S:μ_D ratio and the prevailing force level (Fig. 8c). Given that the normal neuromuscular delay in humans from a slip event to a change in muscle force is 74 ± 9 ms [34], it is encouraging that our three-axial force sensor allows slip detection within 20 ms even at low normal forces and small μ_S:μ_D ratios.

4. Discussion

The goal of this study was to create an artificial tactile system to be embedded in a biomechatronic hand able to convey information believed to be crucial for the successful completion of prototypical manipulation task, viz., to grasp-and-lift an object. It should be emphasized that the developed contact sensor and the three-axial force sensor should be regarded not as precision devices *per se* but rather as part of a system able to extract qualitative or semi-quantitative information of functional significance, as discussed years ago [12,52]. Specifically, the sensors were

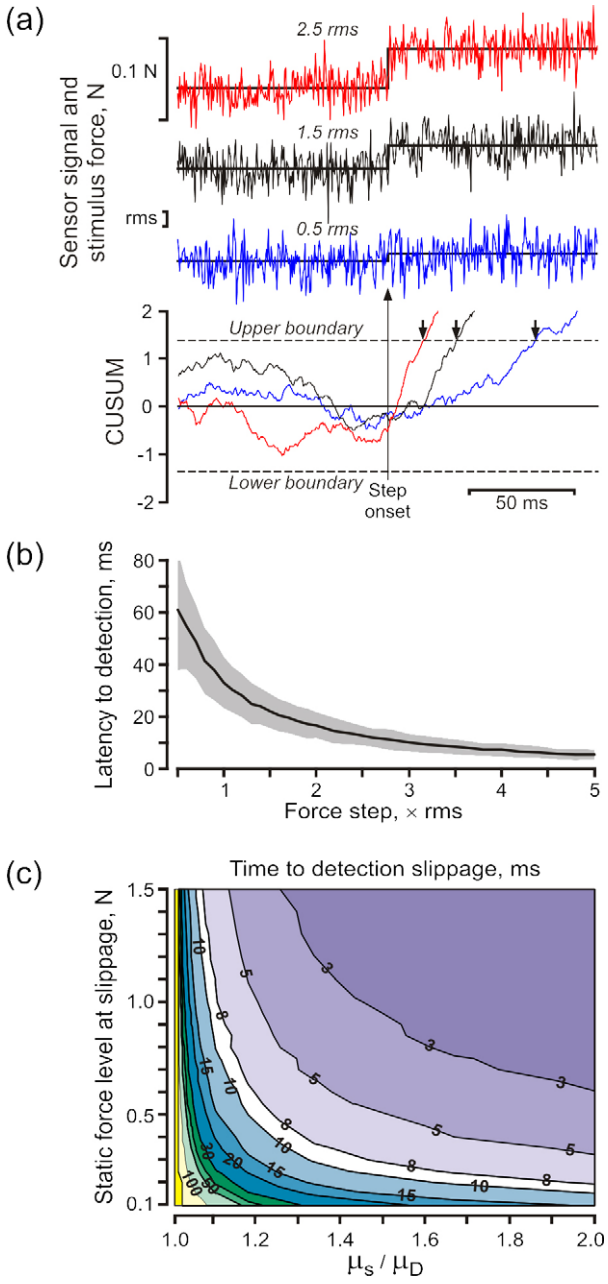

Fig. 8. Detecting force changes. (a) Step changes in the force applied to one of the three sensors of the three-axial force sensor were subjected to a filtering procedure exactly matching the properties of the force sensor and with added noise corresponding to the noise empirically observed. Steps of 0.5, 1.5 and 2.5 × RMS of the sensor signals are shown at the top. The CUSUM represent the cumulated deviations from the mean in a 100 ms windows; the upper and lower boundaries correspond CUSUM values that, given the RMS of the sensors, would be observed by chance about once an hour if the signal was recorded at 2 kHz, and the arrows represent the time at which these boundaries were crossed at the three different levels of force steps. (b) The latency to detection of a sudden change in the force was calculated for a range of force steps. The latency was found to be <20 ms for force steps >1.7 RMS which for the three-axial force sensors corresponded to 0.015 N. (c) The time to detecting slippage depends on the prevailing static force level at slippage and the μ_S/μ_D ratio. The graph shows that the time to detect a slippage using the CUSUM technique would be 15 ms or less for static force levels >0.5 N and μ_S/μ_D ratio >1.1.

designed to allow spatial and temporal identification of contacts between object and the biomechatronic hand and to detect important mechanical transients that occur during the evolution of a typical grasp-and-lift task. While we have characterized the properties of the sensors in these respects, a complete evaluation of the developed sensors in functional tasks was beyond the scope of this study.

The three-axial force sensor was devised to convey information about sudden force changes. We demonstrate that the developed sensor could be used to detect small force changes within a few tens of milliseconds (Figs. 6–8), that is, within the range the information is available in biological systems. The three-axial force sensor thus can be used to detect contact and release of objects as well as interactions between hand-held objects and the environment, and not least importantly, can be used to detect slippage between the fingertips and objects when there is a sizeable difference between the static and dynamic friction (Figs. 6 and 7). But even a six-axial sensor (i.e., linear as well as torsional forces) mounted in the fingertip while able to provide information about the center of contact, cannot by itself provide detailed spatial information about the interaction between even a single fingertip and an object, much less contacts between the various phalanges and the palm and an object. Accordingly, the contact sensor arrays and the three-axial force sensors are complementary devices, as discussed by Melchiorri [49] in the field of robotic dexterous manipulation. In short, it seems reasonable to claim that the contact sensor array together with the three-axial force sensor could be used to provide information about crucial mechanical events that are expected during grasp-and-lift tasks and, as such, be useful for providing critical information to patients wearing prosthetic devices and to robotic systems controlling biomechatronic hands.

Artificial sensors and sensory systems for robotic manipulation have been investigated for decades. Force–torque sensors were developed both fingertip-sized [5,51] and more recently, as micro-fabricated devices [2,54]. Moreover, dynamic tactile sensors, responding only to changes in the conditions at the contact, have been embedded in dexterous robotic manipulators and used to detect mechanical transients, vibrations and slippage [53]. Even though the sensors developed in this study are by no means unique [40], the combined use in an anthropomorphic biomechatronic hand of force sensors, contact sensors and a processing technique well-suited for real-time processing represents, in our opinion, a significant step towards an integrated approach to the design of cybernetic hand prosthesis and to robotic manipulation in general.

A critical factor limiting the convenient use of complex tactile information into real-time controls is represented by the computational requirements of the implemented algorithms [21]. The proposed solution for the processing of sensors signals was conceived from the very beginning to allow easy real-time implementation on current microcontrollers and digital signal processors. Indeed, the electronics for signal acquisition and information extraction could be hosted in the palm of the biomechatronic hand. Importantly, the proposed CUSUM technique to detect 'events' presumes that the controller of the hand is able to predict mechanical events (cf., Fig. 8), an assump-

tion that seems reasonable and will be tested in future studies in which the presented sensor will be used for controlling the mechatronic hand.

The extremely low-noise level of the force sensor and the ability of the CUSUM technique in detecting mechanical transients whose amplitude are as small as 1 × noise RMS within few tens of milliseconds will allow to approach future investigations on incipient slippage in an effective and rigorous way. Several different approaches have been followed, e.g., accelerometers for detecting microvibrations [53], an artificial neural network to detect progressive shape changes of the stress spatial distribution on the sensor surface [6], and dynamic PVDF strips embedded in the ridges of an artificial finger skin [59]; nevertheless correctly identifying incipient slip using an anthropomorphic artificial hand in general grasp-and-lift tasks is still an open research problem.

A crucial aspect in the design of cybernetic prostheses is the way sensorial information is transferred from the biomechatronic device to a user or a patient. It might seem as if the ideal method would be to feed the information through a neural interface. The likelihood of success of such devices appears nowadays still limited given the clinical experience of patients (reviewed in Ref. [45]). Under apparently ideal conditions – resutured accidentally severed nerves and substantial innervation of biological sensors and muscles – the functional results are less than satisfactory unless the patients are in their early teens or younger. An important limiting factor in patients is their ability to plastic change and ability to reinterpret sensory inputs [50]. This limitation also applies to sensory substitution techniques, for instance, by providing feedback by sound or tactile stimuli applied to skin areas that can give rise to conscious perceptions. Importantly, whether feedback is provided cognitively (e.g., verbally), analogously, or by direct neural interfaces its use by patients requires intense training. If, however, the crucial information needed for adequate control of grasping-and-lifting can be identified and in addition – as is indicated by numerous neurophysiological studies – can be represented by temporally discrete signals, training requirements may be reduced.

In addition, the proposed artificial biomimetic tactile system could be helpful for developing and implementing a low-level embedded controller of a biomechatronic hand. This kind of controller might automatically adjusts grasp configuration and forces in a coherent way based on tactile events (static contact, mechanical transients, slippage) and thus leave to the patient only the "high level" control of the device. It is conceivable that such a device would greatly simplify the learning and increase amputee's comfort in using the prosthesis. Event-driven control has been investigated for years in the field of dexterous manipulation [9,22], and finite state machine formalism have been used to model robotic hand controllers based on the ability of the sensory system to isolate mechanical transients [43]. Future work will consist in implementing algorithms for mechanical transients and slippage detection in a real-time hand controller, merging the proprioceptive and exteroceptive information from contact sensor arrays and three-axial force sensors, and allowing investigation not only of sequential but also parallel coordination in manipulation. This line of research will be useful not only for the design of new biomechatronic limbs, but also improve our understanding of and allow testing of proposed biological control paradigms.

Acknowledgements

This work was supported by EU (NEUROBOTICS IST-001917 and the Swedish Research Council (projects 08667 and 2005-6994).

References

[1] M. Basseville, A. Benveniste, Design and comparative study of some sequential jump detection algorithms for digital signals, IEEE Trans. Acoust. Speech Signal Process. 31 (1983) 521–535.
[2] L. Beccai, S. Roccella, A. Arena, F. Valvo, P. Valdastri, A. Menciassi, M.C. Carrozza, P. Dario, Design and fabrication of a hybrid silicon three-axial force sensor for biomechanical applications, Sens. Actuators A 120 (2005) 370–382.
[3] I. Birznieks, M.K. Burstedt, B.B. Edin, R.S. Johansson, Mechanisms for force adjustments to unpredictable frictional changes at individual digits during two-fingered manipulation, J. Neurophysiol. 80 (1998) 1989–2002.
[4] I. Birznieks, P. Jenmalm, A.W. Goodwin, R.S. Johansson, Encoding of direction of fingertip forces by human tactile afferents, J. Neurosci. 21 (2001) 8222–8237.
[5] D. Brock, S. Chiu, Environment perception of an articulated robot hand using contact sensors, Robot. Manuf. Automat. 15 (1985) 89–96.
[6] G. Canepa, R. Petrignano, M. Campanella, D. De Rossi, Detection of incipient object slippage by skin-like sensing and neural network processing, IEEE Trans. Syst. Manuf. Cybern. 28 (1998).
[7] M.C. Carrozza, P. Dario, F. Vecchi, S. Roccella, M. Zecca, F. Sebastiani, The Cyberhand: on the design of a cybernetic prosthetic hand intended to be interfaced to the peripheral nervous system, in: Proceedings of the International Conference on Intelligent Robots and Systems, vol. 3, 2003, pp. 2642–2647.
[8] M.C. Carrozza, C. Suppo, F. Sebastiani, B. Massa, F. Vecchi, R. Lazzarini, M.R. Cutkosky, P. Dario, The SPRING hand: development of a self-adaptive prosthesis for restoring natural grasping, Auton. Robots 16 (2004) 125–141.
[9] M.R. Cutkosky, J.M. Hyde, Manipulation control with dynamic tactile sensing, in: Proceedings of the Sixth International Symposium on Robotics Research, Hidden Valley, PA, 1993.
[10] J. Dargahi, S. Najarian, Human tactile perception as a standard for artificial tactile sensing—a review, Int. J. Med. Robot. Comput. Assist. Surg. 1 (2004) 23–35.
[11] P. Dario, C. Laschi, S. Micera, F. Vecchi, M. Zecca, A. Menciassi, B. Mazzolai, M.C. Carrozza, Biologically-inspired microfabricated force and position mechano-sensors, in: F.G. Barth, T. Secomb, C. Humphrey (Eds.), Sensors and Sensing in Biology and Engineering, Springer-Verlag, Berlin, 2003, pp. 109–125.
[12] P. Dario, R. Lazzarini, R. Magni, An integrated miniature fingertip sensor, in: Proceedings of the Seventh International Symposium on Micro Machine and Human Science, 1996, pp. 91–97.
[13] B.B. Edin, Cutaneous afferents provide information about knee joint movements in humans, J. Physiol. 531 (2001) 289–297.
[14] B.B. Edin, J.H. Abbs, Finger movement responses of cutaneous mechanoreceptors in the dorsal skin of the human hand, J. Neurophysiol. 65 (1991) 657–670.
[15] B.B. Edin, G.K. Essick, M. Trulsson, K.Å. Olsson, Receptor encoding of moving tactile stimuli in humans. I. Temporal pattern of discharge of individual low-threshold mechanoreceptors, J. Neurosci. 15 (1995) 830–847.
[16] B.B. Edin, G. Westling, R.S. Johansson, Independent control of human finger-tip forces at individual digits during precision lifting, J. Physiol. 450 (1992) 547–564.

[17] H.H. Ehrsson, A. Fagergren, T. Jonsson, G. Westling, R.S. Johansson, H. Forssberg, Cortical activity in precision- versus power-grip tasks: an fMRI study, J. Neurophysiol. 83 (2000) 528–536.
[18] H. Forssberg, A.C. Eliasson, H. Kinoshita, R.S. Johansson, G. Westling, Development of human precision grip. I. Basic coordination of force, Exp. Brain Res. 85 (1991) 451–457.
[19] H. Forssberg, H. Kinoshita, A.C. Eliasson, R.S. Johansson, G. Westling, A.M. Gordon, Development of human precision grip. II. Anticipatory control of isometric forces targeted for object's weight, Exp. Brain Res. 90 (1992) 393–398.
[20] C. Häger-Ross, R.S. Johansson, Nondigital afferent input in reactive control of fingertip forces during precision grip, Exp. Brain Res. 110 (1996) 131–141.
[21] R.D. Howe, Tactile sensing and control of robotic manipulation, J. Adv. Robot. 8 (1994) 245–261.
[22] J.M. Hyde, M.R. Cutkosky, A phase management framework for event-driven dextrous manipulation, IEEE Trans. Robot. Autom. 14 (1998) 978–985.
[23] P. Jenmalm, I. Birznieks, A.W. Goodwin, R.S. Johansson, Influence of object shape on responses of human tactile afferents under conditions characteristic of manipulation, Eur. J. Neurosci. 18 (2003) 164–176.
[24] P. Jenmalm, R.S. Johansson, Visual and somatosensory information about object shape control manipulative fingertip forces, J. Neurosci. 17 (1997) 4486–4499.
[25] R.J. Johansson, Å.B. Vallbo, G. Westling, Thresholds of mechanosensitive afferents in human hand as measured with von Frey hair, Brain Res. 184 (1980) 343–351.
[26] R.S. Johansson, Tactile sensibility in the human hand: receptive field characteristics of mechanoreceptive units in the glabrous skin area, J. Physiol. 281 (1978) 101–123.
[27] R.S. Johansson, How is grasping modified by somatosensory input? in: D.R. Humphrey, H.J. Freund (Eds.), Motor Control: Concepts and Issues. Dahlem Konferenzen, John Wiley & Sons Ltd., Chichester, 1991, pp. 331–355.
[28] R.S. Johansson, Sensory control of dexterous manipulations in humans, in: A.M. Wing, P. Haggard, J.R. Flanagan (Eds.), Hand and Brain: The Neurophysiology and Psychology of Hand Movements, Academic Press, San Diego, 1996, pp. 313–381.
[29] R.S. Johansson, I. Birznieks, First spikes in ensembles of human tactile afferents code complex spatial fingertip events Nat. Neurosci. 7 (2004) 170–177.
[30] R.S. Johansson, B.B. Edin, Mechanisms for grasp control, in: A. Pedotti, M. Ferrarin (Eds.), Restoration of Walking for Paraplegics. Recent Advancements and Trends, IOS Press, Amsterdam, 1992, pp. 57–63.
[31] R.S. Johansson, Å.B. Vallbo, Tactile sensibility in the human hand: relative and absolute densities of four types of mechanoreceptive units in glabrous skin, J. Physiol. 286 (1979) 283–300.
[32] R.S. Johansson, Å.B. Vallbo, Spatial properties of the population of mechanoreceptive units in the glabrous skin of the human hand., Brain Res. 184 (1980) 353–366.
[33] R.S. Johansson, G. Westling, Roles of glabrous skin receptors and sensorimotor memory in automatic control of precision grip when lifting rougher or more slippery objects, Exp. Brain Res. 56 (1984) 550–564.
[34] R.S. Johansson, G. Westling, Signals in tactile afferents from the fingers eliciting adaptive motor responses during precision grip, Exp. Brain Res. 66 (1987) 141–154.
[35] R.S. Johansson, G. Westling, Coordinated isometric muscle commands adequately and erroneously programmed for the weight during lifting task with precision grip, Exp. Brain Res. 270 (1988) 1–13.
[36] R.S. Johansson, G. Westling, Programmed and triggered actions to rapid load changes during precision grip, Exp. Brain Res. 271 (1988) 1–15.
[37] R.S. Johansson, G. Westling, Tactile afferent signals in the control of precision grip, in: M. Jeannerod (Ed.), Attention and Performance, Erlbaum, Hilldale, NJ, 1990, pp. 677–713.
[38] R.S. Johansson, G. Westling, Afferent signals during manipulative tasks in man, in: O. Franzén, J. Westman (Eds.), Somatosensory Mechanisms, Macmillan Press, London, 1991, pp. 25–48.
[39] A. Kapandji, The Physiology of the Joints. Upper Limb, vol. 1, Churchill Livingstone, Edinburgh, 1982.
[40] H. Kawasaki, T. Komatsu, K. Uchiyama, Dexterous anthropomorphic robot hand with distributed tactile sensor: Gifu hand II, IEEE Trans. Mechatron. 7 (2002) 296–303.
[41] M. Knibestöl, Stimulus-response functions of rapidly adapting mechanoreceptors in human glabrous skin area, J. Physiol. 232 (1973) 427–452.
[42] M. Knibestöl, Stimulus-response functions of slowly adapting mechanoreceptors in the human glabrous skin area, J. Physiol. 245 (1975) 63–80.
[43] D. Kragic, S. Crinier, D. Brunn, H.I. Christensen, Vision and tactile sensing for real world tasks, in: Proceedings of the 2003 IEEE International Conference on Robotics and Automation, Taipei, Taiwan, 2003.
[44] D. Liu, G. Hirzinger, P. Meusel, A tactile sensing system for the DLR three finger robot hand, in: Proceedings of the International Symposium on Measurement and Control in Robotics, 1995.
[45] G. Lundborg, P. Richard, Bunge memorial lecture. Nerve injury and repair—a challenge to the plastic brain, J. Peripher. Nerv. Syst. 8 (2003) 209–226.
[46] V.G. Macefield, C. Hager-Ross, R.S. Johansson, Control of grip force during restraint of an object held between finger and thumb: responses of cutaneous afferents from the digits, Exp. Brain Res. 108 (1996) 155–171.
[47] B. Massa, S. Roccella, M.C. Carrozza, P. Dario, Design and development of an underactuated prosthetic hand, in: Proceedings of the IEEE International Conference on Robotics and Automation, vol. 4, 2002, pp. 3374–3379.
[48] P.B.C. Matthews, R.B. Stein, The sensitivity of muscle spindle afferents to small sinusoidal changes of length, J. Physiol. 200 (1969) 723–743.
[49] C. Melchiorri, Slip detection and control using tactile and force sensors, IEEE-ASME Trans. Mechatron. 5 (2000) 235–243.
[50] B. Rosén, G. Lundborg, L.B. Dahlin, J. Holmberg, B. Karlson, Nerve repair: correlation of restitution of functional sensibility with specific cognitive capacities, J. Hand Surg. [Br.] 19 (1994) 452–458.
[51] D.L. Salisbury, Interpretation of contact geometries from force measurements, in: M. Brady, R.P. Paul (Eds.), Robotics Research: The First International Symposium, MIT Press, Cambridge, MA, 1984, pp. 240–247.
[52] D. Taddeucci, C. Laschi, L. Lazzarini, R. Magni, P. Dario, A. Starita, An approach to integrated tactile perception, in: Proceedings of the IEEE International Conference on Robotics and Automation, 1997, pp. 3100–3105.
[53] M.R. Tremblay, M.R. Cutkosky, Estimating friction using incipient slip sensing during a manipulation task, in: Proceedings of the IEEE International Conference on Robotics and Automation, 1993, pp. 363–368.
[54] P. Valdastri, S. Roccella, L. Beccai, E. Cattin, A. Menciassi, M.C. Carrozza, P. Dario, Characterization of a novel hybrid silicon three-axial force sensor, Sens. Actuators A 123/124 (2005) 249–257.
[55] Å.B. Vallbo, K.-E. Hagbarth, Activity from skin mechanoreceptors recorded percutaneously in awake human subjects, Exp. Neurol. 21 (1968) 270–289.
[56] Å.B. Vallbo, R.S. Johansson, Properties of cutaneous mechanoreceptors in the human hand related to touch sensation, Hum. Neurobiol. 3 (1984) 3–14.
[57] G. Westling, R.S. Johansson, Factors influencing the force control during precision grip, Exp. Brain Res. 53 (1984) 277–284.
[58] G. Westling, R.S. Johansson, Responses in glabrous skin mechanoreceptors during precision grip in humans, Exp. Brain Res. 66 (1987) 128–140.
[59] D. Yamada, T. Maeno, Y. Yamada, Artificial finger skin having ridges and distributed tactile sensors used for grasp force control, J. Robot. Mechantron. 14 (2002) 140–146.